Magnetoresistive detection of strongly pinned uncompensated magnetization in antiferromagnetic FeMn

Pavel N. Lapa, Igor V. Roshchin, Junjia Ding, John. E. Pearson, Valentine Novosad, J. S. Jiang, and Axel Hoffmann

Phys. Rev. B **95**, 020409 — Published 17 January 2017

DOI: 10.1103/PhysRevB.95.020409

Magnetoresistive detection of strongly pinned uncompensated magnetization in antiferromagnetic FeMn

Pavel N. Lapa,[1, 2] Igor V. Roshchin,[2, 3] Junjia Ding,[1] John. E. Pearson,[1] Valentine Novosad,[1] J. S. Jiang,[1] and Axel Hoffmann[1]

[1]*Material Science Division, Argonne National Laboratory, Argonne, IL 60439, USA*

[2]*Department of Physics and Astronomy, Texas A&M University, College Station, TX 77843-4242, USA*

[3]*Department of Material Science and Engineering, Texas A&M University, College Station, TX 77843-4242, USA*

We observed and studied pinned uncompensated magnetization in an antiferromagnet using magnetoresistance measurements. For this, we developed antiferromagnet-ferromagnet spin valves (AFSV) that consist of an antiferromagnetic layer and a ferromagnetic one, separated by a non-magnetic conducting spacer. In an AFSV, the uncompensated magnetization in the antiferromagnet affects scattering of spin-polarized electrons giving rise to giant magnetoresitance (GMR). By measuring angular dependence of AFSVs resistance, we detected pinned uncompensated magnetization responsible for the exchange bias effect in an antiferromagnet-only exchange bias system Cu/FeMn/Cu. The fact that GMR measured in this system persists up to 110 kOe indicates that the scattering occurs on strongly pinned uncompensated magnetic moments in FeMn. This strong pinning can be explained if this pinned uncompensated magnetization is a thermodynamically stable state and coupled to the antiferromagnetic order parameter. Using the AFSV technique, we confirmed that the two interfaces between FeMn and Cu are magnetically different: The uncompensated magnetization is pinned only at the interface with the bottom Cu layer.

I. INTRODUCTION

A combination of unique properties demonstrated by antiferromagnets[1-3] stimulates the growing interest towards their application in spintronics devices.[4-7] Ability to characterize and tune magnetic properties of antiferromagnets is essential for the future developments in this field. However, there have been much fewer studies of antiferromagnetic materials compared to those of ferromagnets.

Typically, the phenomenological description of a perfect antiferromagnet assumes that the neighboring magnetic moments compensate each other, resulting in a zero total magnetization in the bulk of the antiferromagnet. However, even in a perfect antiferromagnet, the surface can lead to formation of uncompensated magnetization.[8-10] This uncompensated magnetization can play an important role in many mesoscale magnetic phenomena[11] and proximity effects in antiferromagnet-antiferromagnet,[12-14] antiferromagnet-superconductor,[15, 16] and especially antiferromagnet-ferromagnet[17] systems. One of the manifestations of the interaction in antiferromagnet-ferromagnet bilayers is the exchange bias effect.[18-22] Many theoretical models[23-26] of exchange bias assume that some uncompensated magnetization at the interface between a

ferromagnet and an antiferromagnet are pinned after the sample is cooled down through the blocking temperature. This pinned magnetization produces an effective field yielding a shift of the hysteresis loop.[27] Different theoretical models propose different scenarios for the origin of the uncompensated magnetization.

In the simplest scenario, the uncompensated magnetization can happen at a crystal surface where the sublattices are not presented equally, *i.e.*, "uncompensated" surface. This produces a net magnetization due to the dominating sublattice.[9, 28] But even at the nominally "compensated" surface, *i.e.*, when the surface contains equal number of spins from all sublattices, net magnetization forms for certain types of antiferromagnets.[8, 10] In this case, the *surface breaks the symmetry* between the sublattices, introducing an unbalanced magnetization, thus, creating a macroscopic equilibrium state with a net magnetization.[8, 10] Since in both scenarios, the magnetic moments contributing to the uncompensated magnetization are still a part of the antiferromagnetic sublattices, this magnetization is strongly coupled to the bulk antiferromagnetic order. Moreover, reversal of this uncompensated magnetization requires reversal of an entire antiferromagnetic domain. As a result, this magnetization is strongly pinned below the blocking temperature.

Magnetization originating from other sources, *e.g.*, chemical disorder or defects,[19, 20] either at the surface or in the "bulk", where the spins contributing to this magnetization are not an integral part of either of the antiferromagnetic sublattices, and therefore can be pinned or unpinned. If this magnetization is pinned, the pinning happens via interaction with the surrounding magnetic moments in the antiferromagnet. But in this case, even if the antiferromagnet has a high enough anisotropy to create a substantial barrier for reversal of such pinned magnetization, that reversal does not require reversal of an entire antiferromagnetic domain. This is because in this case, on a macroscopic scale, coupling of this magnetization with the antiferromagnetic order parameter does not depend on the sign of this magnetization, and, therefore, the states with the opposite directions of the pinned magnetization have the same energy. As a result, such pinned magnetization can be reversed in a moderate magnetic field.

Typically, the pinned magnetization in an antiferromagnet is a small fraction of the total uncompensated magnetization.[29] This fact makes the detection of the pinned magnetic moment an extremely challenging task. It may seem that the "traditional" SQUID or VSM magnetometry is the most direct technique for the detection.[30] However, for the samples where full magnetic saturation cannot be achieved, it can be hard to untangle reliably the horizontal shift of the hysteresis loop due to the exchange bias and the vertical one due to the pinned magnetization. In such cases, for proper extraction of pinned magnetization magnitude, additional assumptions are required.[31-34] Hence, complementary techniques for detection of the uncompensated magnetization in antiferromagnets, both pinned and unpinned, have been utilized: polarized neutron reflectometry, x-ray dichroism, and anomalous Hall magnetometry.[35-39]

In this manuscript, we demonstrate a new experimental technique that enables to study the pinned uncompensated magnetization while varying temperature and magnetic field. This method relies on the special design of a spin valve that consists of an antiferromagnetic layer and a ferromagnetic one, separated by a thin non-magnetic conducting spacer. The spacer must be thick enough to ensure the absence of an interlayer exchange coupling between the ferromagnet and the antiferromagnet. We call these valves "antiferromagnet-ferromagnet spin valves" (AFSV) to emphasize their difference from the conventional giant magnetoresistance (GMR) spin valves, which are typically composed of two dedicated ferromagnetic layers separated by a conducting spacer.

Similarly to the conventional GMR spin valves, the magnetization in the ferromagnetic layer of AFSV is free, while the pinned uncompensated magnetization in the antiferromagnet is expected to play the role of the fixed ferromagnetic layer. Hence, as in the conventional GMR spin valves, the resistance of an AFSV must depend on the mutual orientation of magnetization in the ferromagnetic layer and the pinned uncompensated magnetization in the antiferromagnet. Consequently, by measuring the angular dependences of the AFSV resistance and subsequently extracting the GMR value, one can obtain information about the direction and magnitude of the pinned magnetization in the antiferromagnet.

It is noteworthy that despite the obvious similarities between conventional GMR spin valves and AFSVs, one significant difference in their operations is expected. In the conventional GMR spin valves, pinning of the fixed layer is usually achieved by exchange biasing the layer with an antiferromagnet. Hence, once the external magnetic field considerably exceeds the exchange bias field, the magnetization in the fixed layer starts reversing. As a result, the GMR significantly decreases in high magnetic fields.[40] In contrast, it is expected that a magnetic field of the order of the interatomic exchange field must be applied to rotate the strongly pinned uncompensated magnetization in the antiferromagnetic layer of AFSVs. Thus, the characteristic feature expected from the AFSVs is that GMR does not vanish even in very high magnetic fields.

Whereas magnetoresistive measurements have been previously used to study uncompensated magnetization in antiferromagnets,[41-43] the focus of those studies and the capabilities of those approaches were different. Our design of AFSV and measuring the angular dependence of its resistance enable us to study pinned magnetization in very high magnetic fields.

II. DETAIL OF THE EXPERIMENT

Previously, we reported the observation of exchange bias in multilayers composed of antiferromagnetic FeMn and diamagnetic Cu.[44] The analysis of the hysteresis loops showed that Cu was responsible for the pinned uncompensated magnetization at the interface between FeMn and Cu. The interaction of pinned and unpinned uncompensated magnetization results in exchange bias, despite the multilayers not having a nominal ferromagnetic layer. The same Cu/FeMn/Cu trilayers were chosen for studying pinning of the uncompensated magnetization using the AFSV technique.

Multilayers with structures Ta(5 nm)/Cu(5 nm)/Py(2 nm)/Cu(5 nm)/FeMn(5 nm)/Cu(5 nm)/Ta(5 nm) and Ta(5 nm)/Cu(5 nm)/FeMn(5 nm)/Cu(5 nm)/Py(2 nm)/Cu(5nm)/Ta(5 nm) are fabricated using magnetron sputtering at room temperature. Permalloy (Py) with the composition $Ni_{0.81}Fe_{0.19}$ is used as a ferromagnetic free layer. Ta/Cu at the bottom and Cu/Ta at the top of the AFSVs are responsible for seeding and for capping, respectively. The deposition rates are 1 Å/sec for Cu, Ta, and Py; and 0.11 Å/sec for FeMn. The AFSVs are cut into stripes with dimensions of 12 mm×2 mm and mounted on a horizontal rotator. Thus, the external magnetic field is kept parallel to the interfacial planes of the spin valves. The current is passed along the long edge of the stripes. In the coordinate system used for the angular-dependence measurements, the zero angle corresponds to the orientation where the long edge of the stripe is parallel to the external magnetic field. A four-probe technique is used for the resistivity measurements (Quantum Design PPMS). Three parameters are varied in the magnetoresistance measurements: the amplitude of the magnetic field during the measurement (H_{MEAS}), the amplitude (H_{COOL}) and the direction (Θ_{COOL}) of the external magnetic field in which the valves are cooled down in preparation for the measurement. To check that the deposition conditions yield Cu/FeMn/Cu with the expected magnetic properties, another multilayer stack with structure Ta(5 nm)/[FeMn(5 nm)/Cu(5 nm)]$_{10}$/Ta(5 nm) is prepared and characterized using magnetometry (Quantum Design SQUID VSM). The hysteresis loop for Ta(5 nm)/[FeMn(5 nm)/Cu(5 nm)]$_{10}$/Ta(5 nm) (Fig. 1) demonstrates the same exchange bias shift and net magnetization as those reported previously.[44]

III. Py/Cu/FeMn/Cu AFSV

The angular dependences of the resistance for the Ta(5 nm)/Cu(5 nm)/Py(2 nm)/Cu(5 nm)/FeMn(5 nm)/Cu(5 nm)/Ta(5 nm) AFSV measured at 10 K in 200 Oe (open dots) and 70 kOe (solid dots) magnetic fields after three different cooling procedures are shown in Fig. 2. According to the first procedure, the AFSV was cooled down from 300 K in 70 kOe magnetic field applied along the long edge of the AFSV (Θ_{COOL}=0°). The angular dependence of resistance measured after this cooling procedure [Fig. 2(a)] has two peaks with maxima at 0° and 180°. It is noteworthy that these peaks are different. For the measurement performed in 200 Oe, the resistance at 0° is 1.6±0.1 mΩ smaller than that at 180°. Overall, for the measurements performed in small (200 Oe) and large (70 kOe) magnetic fields, the angle-dependent part of the resistivity demonstrates harmonic behavior and can be presented as a superposition of two components. The first component is symmetric with respect to reversing the magnetic field, and can be parametrized as cos(2Θ), where Θ is the angle of rotation. This component is due to anisotropic magnetoresistance of Py.[45] The second component describes the asymmetry of the resistance with respect to reversing the magnetic field during the measurement and can be parameterized as cos(Θ). This component is attributed to the GMR effect which is caused by the scattering of electrons polarized by the free Py layer on the uncompensated magnetic moments inside FeMn. To prove that the asymmetry in the peak heights is due to the GMR effect

caused by the pinned uncompensated magnetic moments and it is not an artifact of the measurements such as a drift of the signal, misalignment of the rotation plane and the AFSV plane, the angular dependence of resistance was measured after cooling the valve in 70 kOe magnetic field applied perpendicular to the current direction, *i.e.*, at Θ_{COOL}=90° [Fig. 2(b)], and after zero field cooling [Fig. 2(c)]. Fig. 2(b) demonstrates that changing the direction of the cooling field to Θ_{COOL}=90° yields equal resistances at 0° and 180°, while a difference in resistances at 90° and 270° appears. This is consistent with the proposed mechanism of GMR. Cooling the sample at Θ_{COOL}=90° causes pinning of the uncompensated magnetic moments in this direction, yielding GMR minimum and maximum at 90° and 270°, respectively. Finally, cooling down the AFSV in zero magnetic field [Fig. 2(c)] does not break the symmetry between the opposite directions, and, as a result, GMR is absent. These measurements confirm that the difference between resistances measured when the measurement field is along and opposite to the cooling field, $\Delta R_{\uparrow\downarrow}$, is due to the GMR effect caused by the uncompensated magnetization in FeMn that get pinned after the AFSV is cooled in magnetic field.

As mentioned above, the uncompensated magnetization in FeMn can be divided into two categories: pinned and unpinned. In principle, for the angular dependences obtained in 200 Oe, the asymmetry of peaks could be explained without regard of pinned uncompensated magnetization. It is reasonable to assume that due to local anisotropy, a part of the unpinned uncompensated magnetic moments saturated by a 70 kOe magnetic field cannot be reversed by a modest -200 Oe magnetic field. Hence, these magnetic moments could be responsible for the increased scattering when the AFSV is rotated. At the same time, if the GMR signal were only due to the remanence of the unpinned uncompensated magnetization then the asymmetry would have disappeared when the valve was rotated in high magnetic field. Remarkably, as it can be seen in Fig. 2(a) and (b), the asymmetry is preserved even for the measurements conducted in 70 kOe. Moreover, for the H_{MEAS}=70 kOe measurements, $\Delta R_{\uparrow\downarrow}$=1±0.1 mΩ, which is only 40 % smaller than $\Delta R_{\uparrow\downarrow}$ measured in 200 Oe magnetic field. At this high field, all unpinned uncompensated magnetic moments are aligned along the magnetization of the free Py layer in the 70 kOe magnetic field. This observation confirms that the scattering on the pinned uncompensated magnetization plays the dominant role in the observed GMR effect.

The giant magnetoresistance, $\Delta R_{\uparrow\downarrow}$, in the first approximation, is proportional to the density of scattering centers or pinned uncompensated magnetization. It means that GMR of an AFSV can serve for qualitative and, to some extent, quantitative estimation of pinned uncompensated magnetization at the surface of the antiferromagnet under different conditions: magnetic field, temperature, or field cooling procedure. To evaluate qualitatively how the external magnetic field breaks the pinning of uncompensated magnetization, the Ta(5 nm)/Cu(5 nm)/Py(2 nm)/Cu(5 nm)/FeMn(5 nm)/Cu(5 nm)/Ta(5 nm) AFSV was cooled down from 300 K in 70 kOe magnetic field, and then a set of R(Θ) dependences was

measured at 10 K in different external magnetic fields. The resulting $\Delta R_{\uparrow\downarrow}(H_{MEAS})$ dependence is presented in Fig. 3. As it has been already pointed out, $\Delta R_{\uparrow\downarrow}$ does not go to zero even in 110 kOe magnetic field which confirms the presence of strongly pinned magnetic moments. A naive expectation would be that $\Delta R_{\uparrow\downarrow}$ should decrease more rapidly in higher fields, thus, indicating that the magnetic field breaks the pinning. As it can be seen in Fig. 3, the opposite trend is observed: the slope of $\Delta R_{\uparrow\downarrow}(H_{MEAS})$ decreases after H_{MEAS} exceeds H_{COOL}. Again, the hysteresis loop for the FeMn/Cu multilayer stack (Fig. 1) demonstrates a significant coercive field of 2.3 kOe and, hence, it would be reasonable to assume that upon rotation of the AFSV in 200 Oe even unpinned magnetization could contribute to the scattering, thus increasing $\Delta R_{\uparrow\downarrow}$ at H_{MEAS}=200 Oe. However, this was not observed in the experiment. In our previous work,[44] we showed that that the majority of the pinned uncompensated magnetic moments are located at the interfaces between FeMn and Cu, while the unpinned magnetic moments are uniformly distributed within the FeMn layer. This means that GMR effect in this particular AFSV is mostly caused by the strongly pinned magnetic moments located at the interface, while the unpinned uncompensated magnetic moments in the bulk of the FeMn layer are screened by the surface pinned magnetic moments, and hence, do not significantly affect the electron scattering.

IV. Cu/FeMn/Cu/Py AFSV

Recent combined neutron and x-ray reflectometry study revealed that FeMn is not chemically homogeneous across the FeMn layer thickness.[46] Refinement of the reflectometry data revealed that FeMn located near the interface with the bottom Cu layer has an increased content of Mn. That is, structurally, the top and bottom interfaces with Cu are not identical. Moreover, the comparative magnetometry studies of Cu/FeMn/Cu and FeMn/Cu films has suggested that that the pinning of the uncompensated magnetization happens only at the bottom interface with Cu.[46] To verify this fact, in addition to Py/Cu/FeMn/Cu, the Cu/FeMn/Cu/Py AFSV with Ta(5 nm)/Cu(5 nm)/FeMn(5 nm)/Cu(5 nm)/Py(2 nm)/Cu(5 nm)/Ta(5 nm) structure was fabricated. For this AFSV, most of the scattering should occur at the top FeMn/Cu interface. The same measurement procedures as before were used for this sample. Fig. 4(a) shows the angular dependence of resistance measured at 10 K in 70 kOe after cooling down from 300 K in 70 kOe magnetic field applied along the current direction (Θ_{COOL}=0°). In contrast to the Py/Cu/FeMn/Cu AFSV, where the difference in resistance at 0° and 180° is very pronounced [Fig. 2(a)], for the Cu/FeMn/Cu/Py AFSV, ΔR is present but it is almost an order of magnitude smaller: 0.16±0.1 mΩ [Fig. 4(a) inset].

There could be two possible mechanisms responsible for this weak but non-zero GMR observed in the Cu/FeMn/Cu/Py AFSV. First, a small fraction of the pinned uncompensated magnetization might be in the bulk of the FeMn layer, causing a weak GMR effect. Second, since the thickness of FeMn is only 5 nm which is comparable to the spin diffusion length in this material (1.8±0.5 nm),[47] a small fraction of polarized electrons can penetrate through the FeMn layer, scattering on the

strongly pinned magnetic moments at the bottom, Cu/FeMn interface. To determine which of these two mechanisms are responsible for the scattering, the magnetoresistance of the AFSV as a function of FeMn thickness will be investigated in the future. Even though the exact mechanism of the weak GMR demonstrated by the Cu/FeMn/Cu/Py AFSV is yet to be proven, an order-of-magnitude-smaller GMR for this AFSV, as compared to that for the Py/Cu/FeMn/Cu AFSV, unambiguously proves that the pinned magnetization at the top, FeMn/Cu interface is zero or much smaller than the pinned magnetization at the bottom, Cu/FeMn interface.

IV. CONCLUSION

In summary, a new spin valve technique has been developed and applied to study the pinning of the uncompensated magnetization in the Cu/FeMn/Cu exchange bias system. The special design of the spin valve combined with measuring the angular dependence of the resistance allowed us to demonstrate that the strongly pinned magnetization in antiferromagnetic FeMn cannot be reversed even by applying magnetic field as high as 110 kOe. Persistence of the pinning in high field can be explained only if the pinned uncompensated magnetization originates from the antiferromagnetic sublattices (also discussed in Ref. [46]). This pinned uncompensated magnetization at the Cu/FeMn interface is an equilibrium property of the system and does not originate from defects or other non-equilibrium sources of uncompensated magnetization.[48] Comparison of the magnetoresistances measured for the Py/Cu/FeMn/Cu and Cu/FeMn/Cu/Py AFSVs revealed that strongly pinned uncompensated magnetization forms primarily at the bottom, Cu/FeMn interface. We believe that the proposed AFSV technique can be extremely useful for detection and studies of uncompensated magnetization in antiferromagnets. The proposed technique can be utilized as a platform for development of new antiferromagnet-based spin valves for applications in magnetic field sensors and data storage.

ACKNOWLEDGEMENTS

Work was supported by the Department of Energy Office of Science, Basic Energy Sciences, Material Sciences and Engineering Division. Pavel N. Lapa also received partial support from Texas A&M University. We acknowledge inspiring discussions with K. D. Belashchenko and thank him for critical reading of the manuscript.

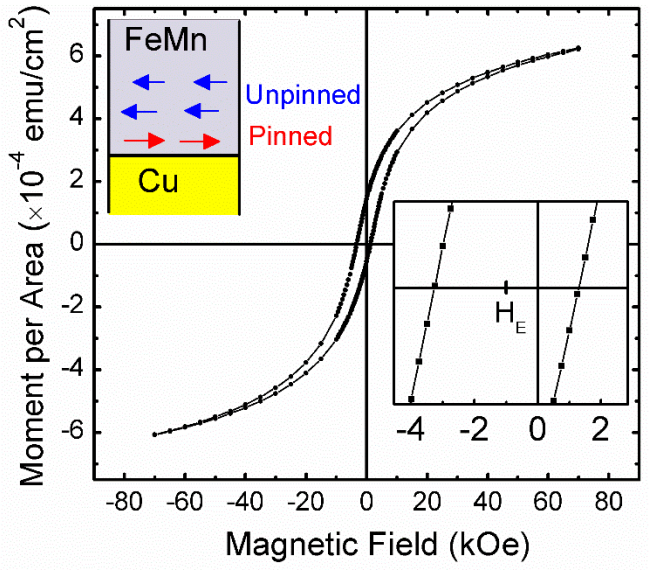

FIG. 1. Magnetic hysteresis loop of the Ta(5 nm)/[Cu(5 nm)/FeMn(5 nm)]$_{10}$/Ta(5 nm) stack measured at 10 K after 70 kOe magnetic field cooling. The bottom-right inset shows the central part of the loop with a clear indication of exchange bias shift. Exchange bias field is H_E=-985 Oe. The top-left inset depicts the pinned and unpinned uncompensated magnetic moments inside the FeMn layer; the compensated antiferromagnetic spin structure is not shown.

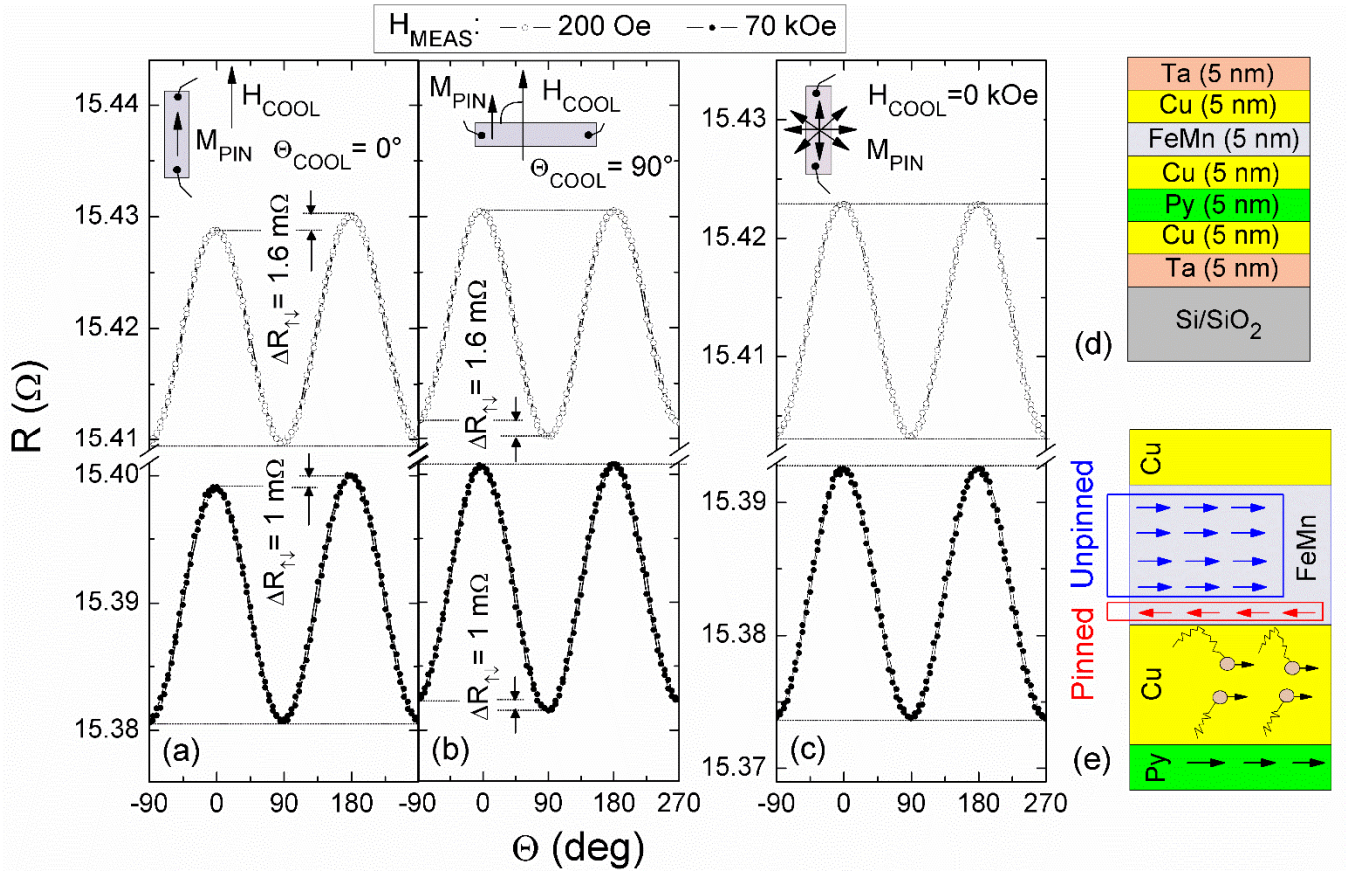

FIG. 2. Angular dependences of resistance of the Ta(5 nm)/Cu(5 nm)/Py(2 nm)/Cu(5 nm)/FeMn(5 nm)/Cu(5 nm)/Ta(5 nm) AFSV measured in 200 Oe (black line/open dots) and 70 kOe (black line/solid dots) after the AFSV was cooled down from 300 K in: a) H_{COOL}=70 kOe, Θ_{COOL}=0°; b) H_{COOL}=70 kOe, Θ_{COOL}=90°; c) H_{COOL}=0 kOe. Zero angle corresponds to the orientation of the AFSV where the current is parallel to the external magnetic field. d) and e) are schematics illustrating the structure of the AFSV and scattering of polarized electrons on pinned uncompensated magnetic moments, respectively.

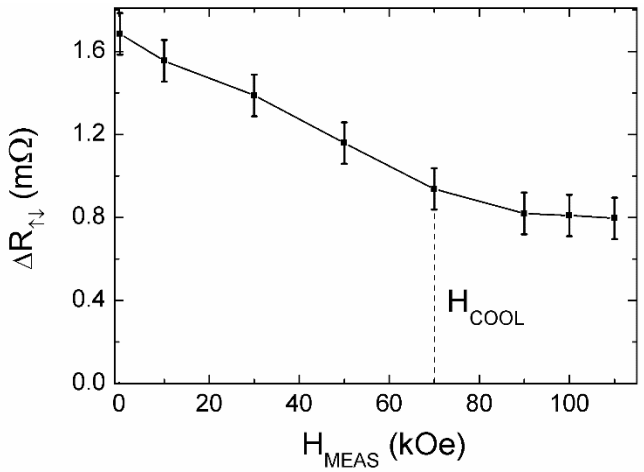

FIG. 3. The difference in resistances measured at 180° and 0°, $\Delta R_{\uparrow\downarrow}$, at T=10 K after field cooling at Θ_{COOL}=0° for the Ta(5 nm)/Cu(5 nm)/Py(2 nm)/Cu(5 nm)/FeMn(5 nm)/Cu(5 nm)/Ta(5 nm) AFSV as a function of magnetic field, H_{MEAS}, applied during the measurement.

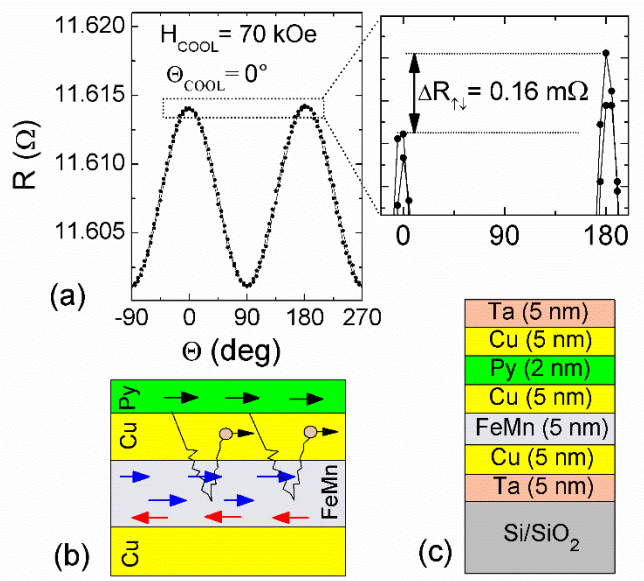

FIG. 4. a) Angular dependence of the resistance of the Ta(5 nm)/Cu(5 nm)/FeMn(5 nm)/Cu(5 nm)/Py(2 nm)/Cu(5 nm)/Ta(5 nm) AFSV measured in 70 kOe after the AFSV was cooled down in: H_{COOL}=70 kOe applied at Θ_{COOL}=0°. The inset in the top right corner shows the magnified peaks. b) and c) are schematics illustrating the scattering of polarized electrons at the Cu/FeMn interface and the structure of the AFSV, respectively.

REFERENCES

1. A. V. Kimel, A. Kirilyuk, A. Tsvetkov, R. V. Pisarev and T. Rasing, Nature **429**, 850-853 (2004).
2. F. Manfred, D. Nguyen Phuc, S. Takuya, B. V. A. Bas, M. Kenjiro, T. Yasuhide and T. Yoshinori, Journal of Physics D: Applied Physics **41**, 164005 (2008).
3. R. Cheng, J. Xiao, Q. Niu and A. Brataas, Physical Review Letters **113**, 057601 (2014).
4. V. Baltz, A. Manchon, M. Tsoi, T. Moriyama, T. Ono and Y. Tserkovnyak, **arXiv:1606.04284**.
5. V. Schuler, K. Olejnik, X. Marti, V. Novak, P. Wadley, R. P. Campion, K. W. Edmonds, B. L. Gallagher, J. Garces, M. Baumgartner, P. Gambardella and T. Jungwirth, **arXiv:1608.03238**.
6. P. Wadley, B. Howells, J. Železný, C. Andrews, V. Hills, R. P. Campion, V. Novák, K. Olejník, F. Maccherozzi, S. S. Dhesi, S. Y. Martin, T. Wagner, J. Wunderlich, F. Freimuth, Y. Mokrousov, J. Kuneš, J. S. Chauhan, M. J. Grzybowski, A. W. Rushforth, K. W. Edmonds, B. L. Gallagher and T. Jungwirth, Science **351**, 587-590 (2016).
7. J. Sklenar, W. Zhang, M. B. Jungfleisch, W. Jiang, H. Saglam, J. E. Pearson, J. B. Ketterson and A. Hoffmann, AIP Advances **6**, 055603 (2016).
8. K. D. Belashchenko, Physical Review Letters **105**, 147204 (2010).
9. M. Charilaou and F. Hellman, Journal of Applied Physics **117**, 083907 (2015).
10. A. F. Andreev, Journal of Experimental and Theoretical Physics Letters **63**, 758-762 (1996).

11. A. C. Basaran, J. E. Villegas, J. S. Jiang, A. Hoffmann and I. K. Schuller, MRS Bulletin **40**, 925-932 (2015).
12. M. Zhongquan, Z. Xiaozhi and C. Xi, Journal of Physics D: Applied Physics **48**, 025002 (2015).
13. A. A. Belik, Inorganic Chemistry **52**, 2015-2021 (2013).
14. S. Mandal, S. Banerjee and K. S. R. Menon, Physical Review B **80**, 214420 (2009).
15. C. Bell, E. J. Tarte, G. Burnell, C. W. Leung, D. J. Kang and M. G. Blamire, Physical Review B **68**, 144517 (2003).
16. M. Hübener, D. Tikhonov, I. A. Garifullin, K. Westerholt and H. Zabel, Journal of Physics: Condensed Matter **14**, 8687 (2002).
17. K. Lenz, S. Zander and W. Kuch, Physical Review Letters **98**, 237201 (2007).
18. H. Ohldag, A. Scholl, F. Nolting, E. Arenholz, S. Maat, A. T. Young, M. Carey and J. Stöhr, Physical Review Letters **91**, 017203 (2003).
19. W. H. Meiklejohn and C. P. Bean, Physical Review **105**, 904-913 (1957).
20. J. Nogués and I. K. Schuller, Journal of Magnetism and Magnetic Materials **192**, 203-232 (1999).
21. R. Morales, Z.-P. Li, J. Olamit, K. Liu, J. M. Alameda and I. K. Schuller, Physical Review Letters **102**, 097201 (2009).
22. M. Finazzi, Physical Review B **69**, 064405 (2004).
23. L. Néel, Annales de physique (Paris) **2**, 61 (1967).
24. A. P. Malozemoff, Physical Review B **35**, 3679-3682 (1987).
25. D. Mauri, H. C. Siegmann, P. S. Bagus and E. Kay, Journal of Applied Physics **62**, 3047-3049 (1987).
26. M. Kiwi, Journal of Magnetism and Magnetic Materials **234**, 584-595 (2001).
27. M. Blamire and B. Hickey, Nature Materials **5**, 87-88 (2006).
28. W. Kuch, L. I. Chelaru, F. Offi, J. Wang, M. Kotsugi and J. Kirschner, Nature Materials **5**, 128-133 (2006).
29. S. Brück, G. Schütz, E. Goering, X. Ji and K. M. Krishnan, Physical Review Letters **101**, 126402 (2008).
30. J. Nogués, C. Leighton and I. K. Schuller, Physical Review B **61**, 1315-1317 (2000).
31. J. B. Tracy, D. N. Weiss, D. P. Dinega and M. G. Bawendi, Physical Review B **72**, 064404 (2005).
32. M. P. Proenca, C. T. Sousa, A. M. Pereira, P. B. Tavares, J. Ventura, M. Vazquez and J. P. Araujo, Physical Chemistry Chemical Physics **13**, 9561-9567 (2011).
33. P. Lv, Y. Zhang, R. Xu, J.-C. Nie and L. He, Journal of Applied Physics **111**, 013910 (2012).
34. J. Geshev, Journal of Magnetism and Magnetic Materials **320**, 600-602 (2008).
35. A. Paul and A. Teichert, Applied Physics Letters **97**, 032505 (2010).
36. M. R. Fitzsimmons, B. J. Kirby, S. Roy, Z.-P. Li, I. V. Roshchin, S. K. Sinha and I. K. Schuller, Physical Review B **75**, 214412 (2007).
37. T. Kosub, M. Kopte, F. Radu, O. G. Schmidt and D. Makarov, Physical Review Letters **115**, 097201 (2015).
38. S. Roy, M. R. Fitzsimmons, S. Park, M. Dorn, O. Petracic, I. V. Roshchin, Z.-P. Li, X. Batlle, R. Morales, A. Misra, X. Zhang, K. Chesnel, J. B. Kortright, S. K. Sinha and I. K. Schuller, Physical Review Letters **95**, 047201 (2005).
39. A. Hoffmann, J. W. Seo, M. R. Fitzsimmons, H. Siegwart, J. Fompeyrine, J. P. Locquet, J. A. Dura and C. F. Majkrzak, Physical Review B **66**, 220406 (2002).
40. Z. Li, Z. Zhang, H. Zhao, B. Ma and Q. Y. Jin, Journal of Applied Physics **106**, 013907 (2009).
41. J. K. Kim, S. W. Kim, K. A. Lee, B. K. Kim, J. H. Kim, S. S. Lee, D. G. Hwang, C. G. Kim and C. O. Kim, Journal of Applied Physics **93**, 7714-7716 (2003).
42. L. Wang, S. G. Wang, S. Rizwan, Q. H. Qin and X. F. Han, Applied Physics Letters **95**, 152512 (2009).
43. B. G. Park, J. Wunderlich, X. Martí, V. Holý, Y. Kurosaki, M. Yamada, H. Yamamoto, A. Nishide, J. Hayakawa, H. Takahashi, A. B. Shick and T. Jungwirth, Nat Mater **10**, 347-351 (2011).
44. D. Kaya, P. N. Lapa, P. Jayathilaka, H. Kirby, C. W. Miller and I. V. Roshchin, Journal of Applied Physics **113**, 17D717 (2013).
45. R. M. Bozorth, Physical Review **70**, 923-932 (1946).
46. P. N. Lapa, A. Glavic, H. Ambaye, V. Lauter, K. D. Belashchenko, T. Eggers, C. W. Miller and I. V. Roshchin, IEEE Magnetics Letters (unpublished).
47. W. Zhang, M. B. Jungfleisch, W. Jiang, J. E. Pearson, A. Hoffmann, F. Freimuth and Y. Mokrousov, Physical Review Letters **113**, 196602 (2014).
48. In contrast, pinned uncompensated magnetization originating from defects is a non-equilibrium state: Due to the random nature of defects, the two configurations with the opposite directions of this magnetization have the same value for the energy term describing macroscopic coupling to the AF order parameter (averaged over the entire sample). As a result, a finite field that is sufficient to overcome uniaxial anisotropy can reverse the direction of this "*pinned*" uncompensated magnetization.